
Signal Propagation in Transformers: Theoretical Perspectives and the Role of Rank Collapse

Anonymous Author(s)

Affiliation

Address

email

Abstract

1 Transformers have achieved remarkable success in several domains, ranging from
2 natural language processing to computer vision. Nevertheless, it has been recently
3 shown that stacking self-attention layers — the distinctive architectural component
4 of Transformers — can result in rank collapse of the tokens’ representations at
5 initialization. The question of if and how rank collapse affects training is still
6 largely unanswered, and its investigation is necessary for a more comprehensive
7 understanding of this architecture. In this work, we shed new light on the causes
8 and the effects of this phenomenon. First, we show that rank collapse of the tokens’
9 representations hinders training by causing the gradients of the queries and keys
10 to vanish at initialization. Furthermore, we provide a thorough description of
11 the origin of rank collapse and discuss how to prevent it via an appropriate depth-
12 dependent scaling of the residual branches. Finally, our analysis unveils that specific
13 architectural hyperparameters affect the gradients of queries and values differently,
14 leading to disproportionate gradient norms. This suggests an explanation for the
15 widespread use of adaptive methods for Transformers’ optimization.

16 1 Introduction

17 Since its first appearance in [Vaswani et al. \[2017\]](#), the Transformer architecture has revolutionized
18 the field of Natural Language Processing (NLP), achieving remarkable success in tasks such as
19 text classification [\[Yang et al., 2019\]](#), machine translation [\[Conneau and Lample, 2019\]](#), reading
20 comprehension [\[Brown et al., 2020\]](#) and question answering [\[Raffel et al., 2019\]](#) among others.
21 Recent efforts have effectively extended its applicability to computer vision [\[Dosovitskiy et al., 2020\]](#)
22 and other domains [\[Baeviski et al., 2020, Huang et al., 2018, Biggio et al., 2021, Polu et al., 2022\]](#),
23 further popularizing it outside NLP.

24 The Transformer operates on inputs comprising a sequence of tokens. At its core, it relies on stacked
25 attention layers, which compute a measure of relevance for the whole sequence by assigning token-
26 wise importance weights — obtained by matrix multiplication of the *queries* and *keys*, and finally
27 normalized with the softmax function. The output of an attention layer is then a linear combination
28 of the importance weights and the so-called *values*. Then, the architecture includes fully-connected
29 sub-layers, residual connections [\[He et al., 2016\]](#), and layer normalization (LN), as illustrated in
30 Fig. 2.

31 In the absence of residual connections, [Dong et al. \[2021\]](#) proved that at initialization the rank of the
32 sequence representation collapses doubly exponentially with depth, and both layer normalization and
33 fully connected layers can only partially alleviate the speed of degeneracy. Under *rank collapse*, the
34 model does not distinguish between representations of different tokens, which are perfectly aligned
35 in feature space at initialization. Crucially, the precise implications of rank collapse in Transformers
36 are not fully understood.

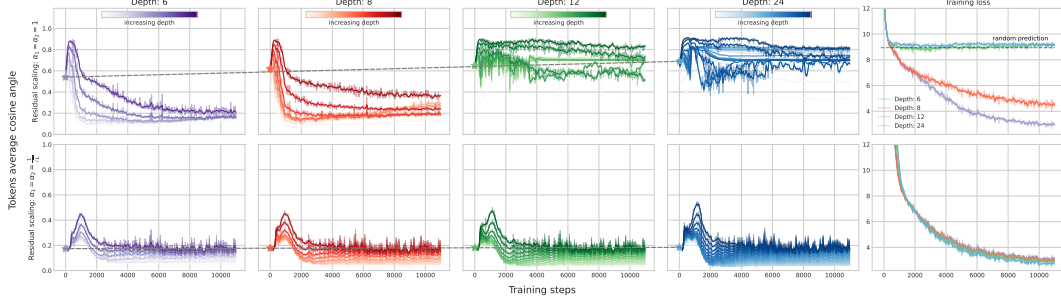


Figure 1: Evolution of the cosine of the angle between tokens for training POST-LN Transformers of increasing depth, with the Adam optimizer, for the IWSLT’14 De-En translation task. Unless adequate residual scaling is used at initialization, increasing depth leads to an increase in the tokens’ alignment at initialization, which can inhibit training.

In this paper, we show that a high alignment of the tokens’ representations at initialization — corresponding to rank collapse in the extreme case of perfect alignment — affects training by causing vanishingly small gradients of the queries and keys’ parameter matrices. This problem severely diminishes the capabilities of the model to learn meaningful attention weights and is further exacerbated in very deep networks, where the rank deficiency — and hence the vanishing gradient problem of the queries and keys — affects several layers (see Fig. 1). In order to shed light on this problem, we take inspiration from the flourishing literature on signal propagation in random networks and start our analysis by computing the expected gradients of an attention layer with respect to the queries, keys, and values, which leads to Theorem 3.2 on the vanishing gradients for the queries and keys. From here, we pursue two different directions.

Firstly, we investigate under which conditions rank collapse can be avoided by studying the evolution of the input sequence in a Transformer at initialization. Our theory reveals that a depth-dependent scaling of the residual branches, beyond stabilizing the norm of the activations at initialization, also approximately preserves the cosine of the angle between tokens, and hence also stabilizes the rank of the propagating sequence. We show that this holds even in the infinite-depth limit.

Secondly, we illustrate that there are factors, other than the average tokens’ correlation, that affect differently the gradient norm of the queries and keys compared to the values. In particular, the propagating sequence’s squared norm has a linear dependence in the values, while a cubic one in the queries and keys, justifying the use of layer normalization. We also highlight a different dependence on the embedding dimension and the length of the input sequence, implying that the gradient norm of a subset of parameters can potentially be of different orders of magnitude, as empirically hinted by previous works [Liu et al., 2020]. Our analysis brings to light fundamental issues in the signal propagation in Transformers, opening the way for new, well-founded and motivated approaches to improve optimization in these models.

2 Background

Transformers. A Transformer architecture consists of L stacked attention blocks, as show in Fig. 2. Layer normalization is usually applied token-wise either after the residual connections or to the inputs of the self-attention and position-wise feed-forward sub-layers, leading to the POST-LN [Vaswani et al., 2017] and PRE-LN [Wang et al., 2019, Xiong et al., 2020] variants respectively.

Formally, given an input sequence $\mathbf{X} \in \mathbb{R}^{n \times d_v}$, with n tokens of dimension d_v , the single-head unmasked scaled dot-product self-attention¹ is defined as:

$$\mathbf{S}^\ell := \mathbf{A}^\ell \mathbf{X}^\ell \mathbf{W}^V, \text{ where } \mathbf{A}^\ell = \text{softmax} \left(\frac{1}{\sqrt{d_k}} \mathbf{X}^\ell \mathbf{W}^Q (\mathbf{X}^\ell \mathbf{W}^K)^\top \right), \quad (1)$$

where the softmax function is applied independently across each row, and the superscript ℓ indexes the ℓ -th layer. The matrices $\mathbf{W}^Q, \mathbf{W}^K \in \mathbb{R}^{d_v \times d_k}$ and $\mathbf{W}^V \in \mathbb{R}^{d_v \times d_v}$ are learnable parameters,

¹Our analysis also easily generalizes to the case of cross-attention.

and each layer is initialized with an independent set of weights. In the literature, the matrices $\mathbf{X}^\ell \mathbf{W}^Q$, $\mathbf{X}^\ell \mathbf{W}^K$, $\mathbf{X}^\ell \mathbf{W}^V$ are referred to as queries, keys and values, respectively. The complete Transformer block, in the absence of layer normalization, can be written recursively as:

$$\mathbf{Z}^\ell = \alpha_1 \mathbf{S}^\ell + \mathbf{X}^\ell \quad (2)$$

$$\mathbf{Y}^\ell = \sigma(\mathbf{Z}^\ell \mathbf{W}^{F_1}) \mathbf{W}^{F_2} \quad (3)$$

$$\mathbf{X}^{\ell+1} = \alpha_2 \mathbf{Y}^\ell + \mathbf{Z}^\ell, \quad (4)$$

where the introduced α_1, α_2 parameters indicate the strength of the residual block, $\mathbf{W}^{F_1}, \mathbf{W}^{F_2} \in \mathbb{R}^{d_v \times d_v}$ ² are matrices of learnable parameters; we set $\mathbf{X}^0 := \mathbf{X}$, and $\sigma : \mathbb{R} \rightarrow \mathbb{R}$ is an activation function. In our case, σ is the ReLU function, but we relax this assumption to the linear activation from Section 3.2 on.

At initialization, each weight is sampled independently from a distribution with zero-mean and variance $\sigma_v^2 = \frac{1}{d_v}$ for the values and feedforward weights³, and $\sigma_k^2 = \frac{1}{d_k}$ for the queries and keys. This is the standard ‘‘Xavier’’ [Glorot and Bengio, 2010] or ‘‘He’’ [He et al., 2015] initialization, commonly used in deep learning.

Rank Collapse in Transformers. Interestingly, Dong et al. [2021] proved that when the residual branches are omitted, the matrix of the tokens’ representations \mathbf{X}^ℓ converges to a rank-1 matrix in which all the representations are the same and equal to a vector $\mathbf{x} \in \mathbb{R}^{d_v}$, i.e. $\mathbf{X}^\ell \rightarrow \mathbf{1}_n \mathbf{x}^\top$, where $\mathbf{1}_{d_v}$ is the vector with all ones in \mathbb{R}^{d_v} . Note that this is a slightly stronger notion of a rank-1 matrix, as it implies that all the tokens’ representations are both perfectly aligned and have the same norm. Indicating the inner product with the usual bracket notations $\langle \cdot, \cdot \rangle$, and the cosine of the angle between two tokens as $\theta_{k,k'}$, perfect alignment happens when $\langle \mathbf{X}_k^\ell, \mathbf{X}_{k'}^\ell \rangle = \|\mathbf{X}_k^\ell\| \|\mathbf{X}_{k'}^\ell\| \cos \theta_{k,k'}$ with $\cos \theta_{k,k'} = 1$ for all $k, k' \in [n]$. Note that perfect alignment together with equal norm between all the tokens implies that all the representations are the same. One of our main contributions is to provide an explanation of how rank collapse affects the gradients of a Transformer at initialization.

Vanishing Gradient Problem. Traditionally considered one of the core issues that prevents successful training, the vanishing gradient problem has a long and rich history that dates back to before the popularization of deep learning [Hochreiter, 1991, Bengio et al., 1994]. In its essence, given a loss function $\mathcal{L} : \mathbb{R}^{n \times d_v} \rightarrow \mathbb{R}$, vanishing gradients occur when the norm of the gradient of the loss \mathcal{L} with respect to the parameters of the network \mathbf{W} — which we indicate as $\|\frac{\partial \mathcal{L}}{\partial \mathbf{W}}\|$ — is too small to provide enough backpropagating signal, thus hindering gradient-based optimization methods. Despite extensive research toward understanding and overcoming the problem in disparate contexts [Glorot and Bengio, 2010, He et al., 2015, Hanin, 2018, Zhang et al., 2019], a formal explanation of its role in relatively new architectures such as Transformers is largely missing in the literature, with a few exceptions [Xiong et al., 2020, Wang et al., 2022, Huang et al., 2020]. In our paper (Section 3.1), we show how vanishing gradient occurs in conjunction with the rank collapse issue identified by Dong et al. [2021].

Signal Propagation in Random Networks at Initialization. After addressing the question on the effects of rank collapse, we take a step back and rigorously analyze its causes by looking at how the properties of the input sequence \mathbf{X} are lost/preserved as it propagates through a randomly initialized Transformer. More specifically, we focus on two aspects of the propagating sequence: the expected

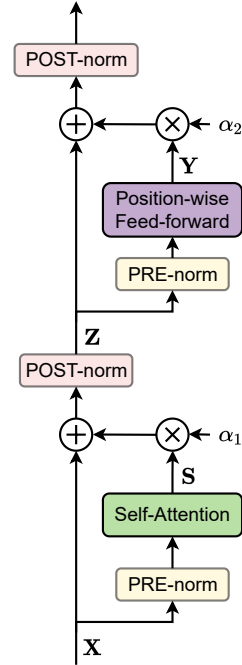


Figure 2: A single Transformer block.

²In practice, one commonly uses $\mathbf{W}^{F_1} \in \mathbb{R}^{d_v \times d_F}$, $\mathbf{W}^{F_2} \in \mathbb{R}^{d_F \times d_v}$ where $d_F = \gamma d_v$, with $\gamma \in \{2, 4, 8\}$. Our results then hold up to a constant factor that depends on γ .

³One should explicitly write the layer dependence $\mathbf{W}^{Q,\ell}, \mathbf{W}^{K,\ell}, \mathbf{W}^{V,\ell}, \mathbf{W}^{F_1,\ell}, \mathbf{W}^{F_2,\ell}$. We at times suppress the ℓ index to improve readability. In case σ is the ReLU function, we set $\mathbf{W}^{F_1,1}$ to have variance $\frac{2}{d_v}$.

113 Frobenius norm $\mathbb{E} \|\mathbf{X}^\ell\|^2$ and the expected inner product between different tokens $\mathbb{E} \langle \mathbf{X}_k, \mathbf{X}_{k'} \rangle$, with
 114 $k \neq k'$. The former is linked to a number of studies on the initialization of neural networks at
 115 the *edge of chaos* [Poole et al., 2016, Schoenholz et al., 2017], and vanishing/exploding gradients
 116 [Hanin, 2018]. The latter quantity describes how the geometry of the feature space changes after
 117 applying a Transformer block, and is related to the concept of *dynamical isometry* [Saxe et al., 2013].
 118 To understand the evolution of the inner product, we analyze the following measure of correlation
 119 [Nachum et al., 2021, Cho and Saul, 2009]:

$$\rho_{kk'}^\ell := \frac{\mathbb{E} \langle \mathbf{X}_k^\ell, \mathbf{X}_{k'}^\ell \rangle}{\sqrt{\mathbb{E} \|\mathbf{X}_k^\ell\|^2 \mathbb{E} \|\mathbf{X}_{k'}^\ell\|^2}}. \quad (5)$$

120 Note that $\rho_{kk'}^\ell = 1$ if and only if the k -th and k' -th tokens are perfectly aligned ($\cos \theta_{kk'} = 1$). We
 121 stress that in our case — differently from the aforementioned works — instead of analyzing the
 122 relationship between two different data points, we study the relationship between tokens of the same
 123 sequence.

124 3 Theoretical Results

125 3.1 Vanishing Gradients for Queries and Keys under Rank Collapse

126 To investigate the problem of vanishing gradients in the attention layers, we make use of the framework
 127 of matrix calculus [Magnus and Neudecker, 2019, Singh et al., 2021]. In particular, we compare
 128 the expected Frobenius norm of the gradient of a self-attention layer with respect to its parameters:

129 $\mathbb{E} \left\| \frac{\partial \mathbf{S}^\ell}{\partial \mathbf{W}} \right\|_F^2$, where here \mathbf{W} indicates one of the keys, queries or values weight matrices. Due to the
 130 well-known difficulty of computing expectations of the softmax [Daunizeau, 2017, Shekhovtsov
 131 and Flach, 2018], throughout this manuscript, we make the simplifying assumption that the softmax
 132 output is the uniform distribution at initialization, i.e. the $n \times n$ matrix containing $\frac{1}{n}$ in each entry.

133 **Assumption 3.1** (Uniform attention). *We assume that $\mathbf{A}^\ell = \frac{1}{n} \mathbf{1}_{n \times n}$,*

134 where $\mathbf{1}_{n \times n}$ is the matrix with all entries equal to 1. Crucially, in Appendix A.5, we formally show
 135 that *this assumption holds almost surely* in the limit $d_k \rightarrow \infty$. There, we also experimentally show
 136 that even in the more realistic case where $d_k = d_v \approx 512$, the empirical simulations provide a
 137 surprisingly faithful approximation of the theoretical insights presented in this paper.

138 We define the mean token $\bar{\mathbf{x}}^\ell$ through its components $\bar{x}_i^\ell = \frac{1}{n} \sum_{k=1}^n \mathbf{X}_{ki}^\ell$, $i \in [d_v]$. In the following
 139 theorem, we compute the expected gradients of an attention layer at initialization, and set the basis
 140 for our following analysis. We provide the results only for the queries, as the case for the keys is
 141 analogous.

Lemma 3.1. *Let \mathbf{X}^ℓ be the representations of the input sequence at the ℓ -th layer. Under the uniform-attention assumption, we have*

$$\mathbb{E} \left\| \frac{\partial \mathbf{S}^\ell}{\partial \mathbf{W}^{V,\ell}} \right\|_F^2 = d_v n \mathbb{E} \|\bar{\mathbf{x}}^\ell\|^2; \quad (6)$$

$$\mathbb{E} \left\| \frac{\partial \mathbf{S}^\ell}{\partial \mathbf{W}^{Q,\ell}} \right\|_F^2 = \frac{\sigma_v^2 \sigma_k^2 d_v}{n^2} \cdot \mathbb{E} [\|\mathbf{X}^\ell\|_F^2 \cdot \|\mathbf{X}^\ell\|_F^2 - n \bar{\mathbf{x}}^\ell (\bar{\mathbf{x}}^\ell)^\top \|\mathbf{X}^\ell\|_F^2]; \quad (7)$$

$$\mathbb{E} \left\| \frac{\partial \mathbf{S}^\ell}{\partial \mathbf{X}^\ell} \right\|_F^2 \leq \frac{8 \sigma_q^2 \sigma_k^2 \sigma_v^2 d_k d_v}{n} \cdot \mathbb{E} \|\mathbf{X}^\ell\|_F^2 - n \bar{\mathbf{x}}^\ell (\bar{\mathbf{x}}^\ell)^\top \|\mathbf{X}^\ell\|_F^2 + 2 d_v^2 \sigma_v^2. \quad (8)$$

142
 143 We defer the precise study of the scaling of these quantities as a function of n and d_v, d_k , to Section 3.3.
 144 At this stage, it is crucial to note that $\frac{1}{n} (\mathbf{X}^\ell)^\top \mathbf{X}^\ell - \bar{\mathbf{x}}^\ell (\bar{\mathbf{x}}^\ell)^\top$ is the centered empirical covariance
 145 matrix of the tokens' representations. It is easy to see that if \mathbf{X}^ℓ is a rank-1 matrix, then all the rows
 146 of \mathbf{X}^ℓ are proportional to a fixed d_v -dimensional vector, and the empirical covariance matrix has
 147 all zero entries. Introducing a loss function $\mathcal{L} : \mathbb{R}^{n \times d_v} \rightarrow \mathbb{R}$, we make the statement on vanishing
 148 gradients more formal in the following theorem:

Theorem 3.2 (Vanishing gradients under rank collapse). *Suppose that the uniform-attention assumption holds. If additionally \mathbf{X}^ℓ for any $l \in [L]$ has rank-1, and there exists a vector $\mathbf{x} \in \mathbb{R}^d$ such that $\mathbf{X}^\ell = \mathbf{1}_n \mathbf{x}^T$, then:*

$$\mathbb{E} \left\| \frac{\partial \mathcal{L}}{\partial \mathbf{W}^{Q,\ell}} \right\|_F^2 = 0, \quad \mathbb{E} \left\| \frac{\partial \mathcal{L}}{\partial \mathbf{W}^{K,\ell}} \right\|_F^2 = 0, \quad (9)$$

where the expectation is taken over the weight matrices. This implies that these quantities are vanishing almost surely, due to the non-negativeness of the norm.

The proof simply relies on expanding the norm of the gradient of the loss with the aid of the chain rule and then bounding it by the product of the norms of each term of the chain. The final result holds with an application of Lemma 3.1, in which the rank-1 assumption makes $\mathbb{E} \left\| \frac{\partial \mathbf{S}^\ell}{\partial \mathbf{W}^{Q,\ell}} \right\|$ vanish.

In light of Theorem 3.2, we can conclude that the rank collapse issue originally identified in Dong et al. [2021] corresponds to an initialization in a region of vanishing gradient signal in the subspace of parameters identified by the queries and keys. How can this affect training? One may argue that if rank collapse does not happen in the very first layer, then the corresponding gradients are non-zero, and the rank of the subsequent layers — affected by rank collapse — can be increased with the first few steps of gradient descent. In practice, we show empirically in Fig. 1 that escaping this pathological landscape is harder in deeper nets.

3.2 Forward Signal Propagation and the Importance of Scaling the Residual Branches

We now turn our attention to the study of the influence of skip connections in transformers. Dong et al. [2021] showed that simply adding skip connections prevents rank collapse. Somewhat surprisingly, we show that while the claim holds for any finite depth, the average angle between different tokens quickly increases with just a few layers, and as $L \rightarrow \infty$ a Transformer can still lose rank unless the residual branches are adequately initialized. As Dong et al. [2021] showed that layer normalization does not avoid rank collapse, we omit it in our analysis. Firstly, we introduce two lemmas on the propagation of inner products (Lemma 3.2) and the norm (Lemma 3.3) of the tokens' representations.

Lemma 3.2 (Propagation of inner products). *Let $C(\mathbf{X}^\ell) = \sum_{k,k'} \langle \mathbf{X}_k^\ell, \mathbf{X}_{k'}^\ell \rangle$ and \mathbf{X} the input sequence. Under the Assumption 3.1 and if σ is the linear activation function, we have that:*

$$\mathbb{E} [C(\mathbf{X}^L)] = (\alpha_2^2 + 1)^L (\alpha_1^2 + 1)^L C(\mathbf{X}). \quad (10)$$

hence, under the depth scaling for the residual block parameters $\alpha_1^2 = \frac{\tilde{\alpha}_1}{L}, \alpha_2^2 = \frac{\tilde{\alpha}_2}{L}$ with $\tilde{\alpha}_1, \tilde{\alpha}_2 \in \mathbb{R}$ independent of L , we have that:

$$\lim_{L \rightarrow \infty} \mathbb{E}[C(\mathbf{X}^L)] = e^{\tilde{\alpha}_1 + \tilde{\alpha}_2} C(\mathbf{X}). \quad (11)$$

Note that $C(\mathbf{X}^\ell) = n^2 \|\bar{\mathbf{x}}^\ell\|^2$. The lemma on the propagation of the norm is slightly more involved:

Lemma 3.3 (Propagation of the norm). *Let \mathbf{X}^L be the representations of the input sequence at the final layer. Under the assumptions of Lemma 3.2, we have that:*

$$\mathbb{E} \|\mathbf{X}^L\|_F^2 = n(\alpha_2^2 + 1)^L \alpha_1^2 \sum_{k=0}^{L-1} (\alpha_1^2 + 1)^k \|\bar{\mathbf{x}}\|^2 + (\alpha_2^2 + 1)^L \|\mathbf{X}\|_F^2, \quad (12)$$

hence, under the depth scaling for the residual block parameters $\alpha_1^2 = \frac{\tilde{\alpha}_1}{L}, \alpha_2^2 = \frac{\tilde{\alpha}_2}{L}$ with $\tilde{\alpha}_1, \tilde{\alpha}_2 \in \mathbb{R}$ independent of L , we have that:

$$\lim_{L \rightarrow \infty} \mathbb{E} \|\mathbf{X}^L\|_F^2 = n e^{\tilde{\alpha}_2} (e^{\tilde{\alpha}_1} - 1) \|\bar{\mathbf{x}}\|^2 + e^{\tilde{\alpha}_2} \|\mathbf{X}\|_F^2. \quad (13)$$

The proof of Lemma 3.3 consists in expanding $\mathbb{E} \|\mathbf{X}^L\|_F^2$ according to the defining equations for the Transformer, and simplifying the expression by using iterated expectations $\mathbb{E} \|\mathbf{X}^L\|_F^2 =$

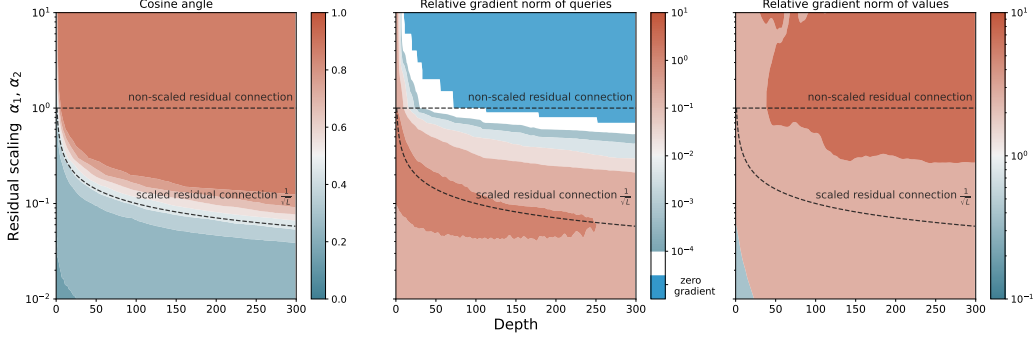


Figure 3: Effect of the residual scaling to the norm of the gradients of the network at initialization with respect to some loss. From left to right: (a) the cosine of the angle between tokens increases with depth. Note how larger values of α_1, α_2 imply a faster token alignment with depth (Theorem 3.3). Subplots (b) and (c) show the gradients of the queries-keys and values parameters respectively by increasing depth, compared to the corresponding norms of the first layer. Gradients for the queries-keys diminish with depth, while the opposite happens for the values. We use POST-LN to disentangle the effect of the variance of the input.

173 $\mathbb{E}[\mathbb{E}[\|\mathbf{X}^L\|_F^2 | \mathbf{X}^\ell]]$ to exploit the conditional independence between different layers, and then computing the expectations using the independence assumption on the weights. The expression on the right-hand side will then depend on \mathbf{X}^ℓ only through its norm $\|\mathbf{X}^\ell\|$ and the norm of the mean token $\|\bar{\mathbf{x}}^\ell\|^2$. Using Lemma 3.2 then allows us to unroll the recursion and get the final result. The complete proof, together with the proof of Lemma 3.2, can be found in Appendix A.3.

178 The previous Lemma provides theoretical justification that scaling the residual branches by setting the alpha parameters to be $\mathcal{O}(1/\sqrt{L})$ allows both the norm of the propagating input and the inner products between different tokens to be approximately preserved. Hence, the information contained in the input is not lost, even in the infinite depth limit.

182 **Residual Scaling Preserves Correlations.** We now prove that without the depth-dependent residual scaling (i.e. with $\alpha_1 = \alpha_2 = 1$) the correlation between the tokens quickly increases, and reaches perfect alignment in the infinite depth limit. More specifically, our argument shows that in this limit, the correlation between different tokens $\rho_{k,k'}^\ell$ as in Eq. (5) converges to 1, implying rank collapse. Furthermore, we show how setting the residual parameters α_1 and α_2 as dictated by Theorem 3.3, ensures that the correlation measure is dependent on the input in a non-trivial way even at infinite depth. To this end, we introduce the average correlation at layer ℓ :

$$\rho^\ell = \frac{1}{n(n-1)} \sum_{k \neq k'} \rho_{kk'}^\ell. \quad (14)$$

189 Note that $\rho^\ell = 1$ if and only if every pair of tokens is perfectly aligned. We are now ready to formalize the influence of the $1/\sqrt{L}$ -scaling on the correlation between tokens' representations by stating Theorem 3.3.

Theorem 3.3. *Let the input tokens have the same norm, i.e. $\|\mathbf{X}_k\| = \|\mathbf{x}\| \ \forall k \in [n]$ for some $\mathbf{x} \in \mathbb{R}^{d_v}$. Under the depth scaling for the residual block parameters $\alpha_1^2 = \frac{\tilde{\alpha}_1}{L}, \alpha_2^2 = \frac{\tilde{\alpha}_2}{L}$ with $\tilde{\alpha}_1, \tilde{\alpha}_2 \in \mathbb{R}$ independent of L , we have that:*

$$\lim_{L \rightarrow \infty} \rho^\ell = \frac{ne^{\tilde{\alpha}_1} C(\mathbf{X})}{(n-1)[(e^{\tilde{\alpha}_1} - 1)C(\mathbf{X}) + n\|\mathbf{X}\|_F^2]} - \frac{1}{n-1}. \quad (15)$$

On the other hand, if $\alpha_1, \alpha_2 \neq 0$ are some constants independent of L , we have that:

$$\lim_{L \rightarrow \infty} \rho^\ell = 1. \quad (16)$$

192

The proof consists in noting that due to the symmetry of the problem at initialization, for a fixed layer the expected norm of each token is the same. Hence, by our definition of $\rho_{kk'}^\ell$, we can write $\mathbb{E}\langle \mathbf{X}_k^\ell, \mathbf{X}_{k'}^\ell \rangle = \rho_{kk'}^\ell \mathbb{E} \|\mathbf{x}^\ell\|^2$. By summing over the k, k' indexes, the resulting equation will depend on $\mathbb{E}[C(\mathbf{X}^\ell)]$ and $\mathbb{E} \|\mathbf{X}^\ell\|^2$, which can be expanded using Lemma 3.2 and 3.3 respectively. The result is then given by solving for ρ^ℓ .

Note that under the $1/\sqrt{L}$ -scaling, the correlation term is one if and only if $C(\mathbf{X}) = n \|\mathbf{X}\|^2$, which holds in the degenerate case where all the input tokens are perfectly aligned. In Appendix A.4, we give precise formulas for the expected correlations at any depth, showing that ρ^ℓ reaches values close to one even for relatively shallow networks when the $1/\sqrt{L}$ -scaling is not adopted (see also Fig. 3 (left)). Additionally, in Fig. 4, we empirically show that in the presence of the $1/\sqrt{L}$ -scaling, layer normalization (either PRE or POST) does not significantly affect the evolution of the correlations. On the other hand, without the residual scaling, PRE-LN seems to alleviate the rate of increase of $\rho_{kk'}^\ell$. It is intriguing that most deep Transformer models use this configuration [Brown et al., 2020]. We provide more extensive empirical results in Appendix B.

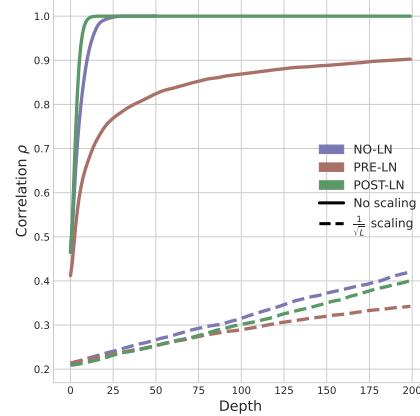


Figure 4: Evolution of Correlation in Transformers with (dashed lines) and without (solid lines) $1/\sqrt{L}$ -scaling for PRE-LN, POST-LN and without layer normalization (No-LN).

Note that the $1/\sqrt{L}$ scaling for the residual branches has been previously studied in the context of stabilization of residual networks (see Section 4), here we extend these results to Transformers and provide new insights on its role in the context of rank preservation. Finally, note that by setting $\tilde{\alpha}_1, \tilde{\alpha}_2 = 0$, we recover the so called "ReZero" initialization [Bachlechner et al., 2021]. In this context, the $1/\sqrt{L}$ scaling extends this framework as it allows for wider range of values for $\tilde{\alpha}_1, \tilde{\alpha}_2$ while still guaranteeing stability.

ReLU extension. We mention here that extending these results from the linear activation to the ReLU case is known to be a hard problem, due to the technical difficulty of propagating the inner products across ReLU layers that are shared among the tokens (this is the case in the position-wise feed-forward layers in Transformers). Exact formulas can be found only in the case of one ReLU layer with Gaussian inputs in Cho and Saul [2009]. However, in the context of rank collapse analyzed here, the linear activation function provides a bound on the correlation with respect to the ReLU case. In fact, correlations are exactly preserved in expectation in the linear case, but increase in the ReLU case (for instance, see the contraction argument in Nachum et al. [2021] below Equation (2)). Hence, the perfect alignment (a.k.a rank collapse) that affects the linear case affects the ReLU case as well (in which case the rank collapses even faster with depth, as we show in Figure 10).

3.3 Dependence on the Angle between Tokens and the Input Norm

In this section, we drop the superscript ℓ as it is obvious from context and assume for simplicity that $d_k = d_v$. To gain a better intuition on the factors that affect the gradients and provide additional insights, we study the case in which every pair of distinct tokens are zero-mean Gaussian random variables, correlated in the same way, i.e $\rho_{ii'}^\ell = \rho$ for $i \neq i'$ or more precisely

$$\mathbb{E}[\mathbf{X}_{i,j} \mathbf{X}_{i',j'}] = \begin{cases} 0 & j \neq j' \text{ (independent dimensions)} \\ \sigma_x^2 & i = i', j = j' \\ \rho \sigma_x^2 & i \neq i', j = j' \end{cases}.$$

To see that this equation satisfies our definition of the correlation metric, note that $\mathbb{E}[\|\mathbf{X}_i\|^2] = d\sigma_x^2$ and $\mathbb{E}\langle \mathbf{X}_i, \mathbf{X}_{i'} \rangle = d\sigma_x^2 \rho$, for $i \neq i'$. Then, the expected norm of the gradients for the values (Eq. (6)) simplifies to

$$\mathbb{E} \left\| \frac{\partial \mathbf{S}}{\partial \mathbf{W}^V} \right\|_F^2 = \sigma_x^2 d^2 (1 + \rho(n-1)). \quad (17)$$

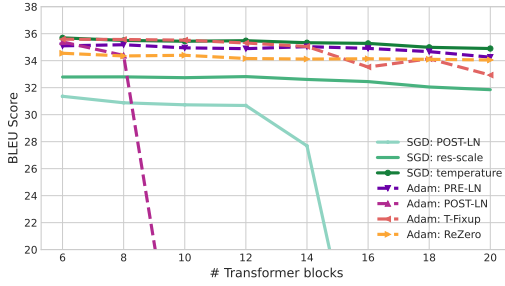


Figure 5: BLEU scores by increasing the number of transformers blocks. ‘X’ Transformer blocks implies in total ‘X’ encoder self-attention, ‘X’ decoder self-attention and ‘X’ decoder cross-attention layers.

Table 1: BLEU scores for the IWSLT14 German-to-English translation task. *SGD res-scale* refers to the training of SGD without layer normalization and initialization of the residual scaling $a_1 = a_2 = \frac{1}{\sqrt{L}}$. *SGD temperature* additionally employs an inverse temperature inside the softmax.

Method (6L-Encoder / 6L-Decoder)	BLEU \uparrow
SGD POST-LN	31.36
SGD res-scale	32.79
SGD temperature	35.69
Adam POST-LN [Vaswani et al., 2017]	35.39
Adam PRE-LN [Vaswani et al., 2017]	35.10
ReZero [Bachlechner et al., 2021]	34.55
T-Fixup [Zhang et al. [2019]	35.59

By making the additional assumption that the norm and the correlation propagate independently, the respective norm for the queries — and symmetrically the keys — (Eq. (7)) reduces to:

$$\mathbb{E} \left\| \frac{\partial \mathbf{S}}{\partial \mathbf{W}^Q} \right\|_F^2 = \sigma_x^6 \frac{(n-1)}{n} (1-\rho)^2 d(n+d). \quad (18)$$

In Appendix A.2 we provide a rigorous proof, that relies on Isserlis theorem [Isserlis, 1918] to compute higher-order moments. The above expressions reveal the different dependencies on four main actors, that we inspect separately here. The gradients of the queries depend via a cubic function on the *variance of the input*, σ_x^2 , compared to a linear for the values. This provides an additional interpretation of the successful use of layer normalization, as in Xiong et al. [2020], either in the POST-LN or PRE-LN format, that standardizes the input variance σ_x^2 to the value 1.

Next, we emphasize the dependence on the *correlation between the tokens*, also illustrated in Fig. 3. Importantly, note how the queries/keys have opposite monotonic functional dependence with respect to ρ compared to the values. As revealed by Theorem 3.3 and Fig. 3 (center), inappropriate scaling of the residual branches can already lead to this phenomenon even in a relatively shallow network.

Finally, Eq. (17) and (18) reveal a different scaling in terms of the *embedding size* d and the *sequence length* n due to the self-attention operation itself. We hope that the identification of the different dependencies in the gradients of the parameters will inspire a new line of works aimed at solving some of the difficulties in training Transformers.

3.4 Are Adaptive Methods really needed for training Transformers?

The existence of the discrepancy in the magnitude of the gradients with respect to the weights \mathbf{W}^Q , \mathbf{W}^K and \mathbf{W}^V , might explain the success of adaptive optimization algorithms, as illustrated in Fig. 6, where we plot the effective learning rate computed by Adam [Kingma and Ba, 2014] in a toy encoder task (more details in Appendix C). Hence, we embark on a preliminary exploration to train a Transformer architecture with SGD with the intent of matching Adam’s performance. Based on our theory, we propose a simple architectural modification, an inverse temperature scaling $\tau \in \mathbb{R}$ inside the softmax:

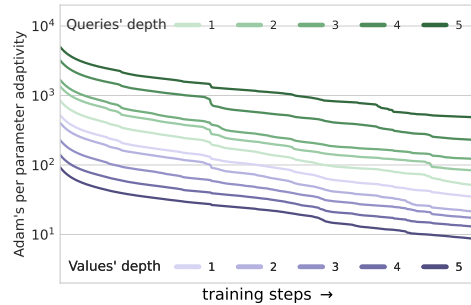


Figure 6: Adaptive learning rates computed by Adam in Transformers.

$$\mathbf{S}_\tau^\ell := \text{softmax} \left(\frac{\tau}{\sqrt{d_k}} \mathbf{x}^\ell \mathbf{W}^Q (\mathbf{x}^\ell \mathbf{W}^K)^\top \right) \mathbf{x}^\ell \mathbf{W}^V. \quad (19)$$

A direct consequence of our analysis is that τ allows controlling the magnitude of the gradients for the queries and keys’ parameters. In Section C.2, we detail how one can choose τ such that the magnitude of the gradients as derived in Equation 17 and 18 is approximately matched at initialization.

We evaluate our proposal, consisting of residual scaling and the aforementioned inverse temperature parameters, on the widely used IWSLT14 German-to-English (De-En) benchmark translation task. All details regarding the experimental setup and the choice of inverse temperature used are provided in Appendix C. We train a Transformer encoder-decoder of varying depth with SGD, after removing all normalization layers and adequately initializing the residual connections. For our training with SGD, we avoid using any learning rate warm-up, as commonly done for Adam, and instead use a step-scheduler to decrease the learning rate at 40% and 80% of training. We compare against the following methods that make use of Adam; POST-LN and PRE-LN refer to the aforementioned alternatives to apply layer normalization. We also compare against other successful techniques that rely on specific initializations to avoid layer normalization, such as ReZero [Bachlechner et al., 2021] and T-Fixup [Zhang et al., 2019]. We report the average BLEU score [Papineni et al., 2002] across 5 runs in Fig. 5 and Table 1.

Our proposed method considerably improves training with SGD, keeping up and in some cases surpassing any results achieved by the Adam optimizer. We are also able to train deeper networks without the use of layer normalization. We leave for future work to further investigate modifications or alternatives to the self-attention operation.

4 Related Work

Our work builds upon the rich literature on forward and backward signal propagation in random neural networks [Poole et al., 2016, Schoenholz et al., 2017, Xiao et al., 2018, Pennington et al., 2017, Orvieto et al., 2021, Noci et al., 2021, Zavatone-Veth and Pehlevan, 2021]. The $1/\sqrt{L}$ scaling scheme has been investigated in the literature for the stabilization of residual networks [Hanin and Rolnick, 2018, Arpit et al., 2019, Allen-Zhu et al., 2019, Hayou et al., 2021].

Our work draws inspiration from a series of recent works studying the rank of the representations of random feed-forward neural networks at initialization [Daneshmand et al., 2020, 2021]. In the context of Transformers, Dong et al. [2021] has recently identified the rank collapse issue object of study of the present work. Thanks to our analysis of the backward pass, we are able to demonstrate that rank collapse in Transformer architectures leads to vanishingly small gradients of queries and keys, thereby preventing effective training and allowing us to complete the analysis of [Dong et al., 2021].

Among the architectural components in Transformers, layer normalization is, arguably, one of the most important – and debated – ones [Chen et al., 2018, Wang et al., 2019, Nguyen et al., 2010, Xiong et al., 2020]. In the original architecture [Vaswani et al., 2017], layer normalization is used to stabilize the forward pass by reducing the variance of the inputs to the following sublayer. Our analysis of the forward pass shows that its inclusion is not strictly necessary for the purpose of controlling the norm of the representations. For a theoretical analysis of signal propagation in the presence of layer norm, we refer the reader to Xiong et al. [2020].

Additionally, our theoretical study of the backward pass provides a rigorous explanation of the empirically observed discrepancy between the magnitude of the gradients of the queries and the values, which Liu et al. [2020] hypothesize to be one of the causes of the success of adaptive methods in training Transformers [Liu et al., 2019, Zhang et al., 2020, Huang et al., 2020].

Finally, properly rescaled residual connections have been found to be beneficial for training Transformers by a number of recent research works [Zhang et al., 2019, Bachlechner et al., 2021, Wang et al., 2022]. However, none of these studies characterize the impact of skip connections on rank propagation, while our analysis suggests a theoretically-grounded way to stabilize it.

5 Conclusions and Future Work

In this paper, we showed how, at initialization, rank collapse and more generally high correlation in the tokens, causes vanishing gradients of the queries and keys of a Transformer architecture. While residual connections help mitigate rank collapse at finite depth, we showed that they alone cannot prevent high alignments of the tokens’ representations — unless properly scaled by a $1/\sqrt{L}$ -factor. Finally, we have also discovered counter-intuitive dependencies on the variance of the input, embedding size, and sequence length, potentially causing large differences between the gradients

of queries/keys compared to the values’ parameters. Hence, we conclude that one of the strengths of Transformers lies in their carefully designed architecture together with an adequate initialization. Finally, we gave preliminary evidence that one of the factors contributing to the higher efficacy of Adam compared to SGD in training Transformers arises from the disproportionate magnitude of gradients as postulated by our theory. Nonetheless, other factors might further accentuate the difference between these two algorithms during training, leaving the door open for further research regarding the benefits of adaptive optimization methods with Transformers.

References

- Zeyuan Allen-Zhu, Yuanzhi Li, and Zhao Song. A convergence theory for deep learning via over-parameterization. In *International Conference on Machine Learning*, pages 242–252. PMLR, 2019.
- Devansh Arpit, Víctor Campos, and Yoshua Bengio. How to initialize your network? robust initialization for weightnorm & resnets. *Advances in Neural Information Processing Systems*, 32, 2019.
- Thomas Bachlechner, Bodhisattwa Prasad Majumder, Henry Mao, Gary Cottrell, and Julian McAuley. Rezero is all you need: Fast convergence at large depth. In *Uncertainty in Artificial Intelligence*, pages 1352–1361. PMLR, 2021.
- Alexei Baevski, Yuhao Zhou, Abdelrahman Mohamed, and Michael Auli. wav2vec 2.0: A framework for self-supervised learning of speech representations. *Advances in Neural Information Processing Systems*, 33:12449–12460, 2020.
- Yoshua Bengio, Patrice Simard, and Paolo Frasconi. Learning long-term dependencies with gradient descent is difficult. *IEEE transactions on neural networks*, 5(2):157–166, 1994.
- Luca Biggio, Tommaso Bendinelli, Alexander Neitz, Aurelien Lucchi, and Giambattista Parascandolo. Neural symbolic regression that scales. In *International Conference on Machine Learning*, pages 936–945. PMLR, 2021.
- Tom Brown, Benjamin Mann, Nick Ryder, Melanie Subbiah, Jared D Kaplan, Prafulla Dhariwal, Arvind Neelakantan, Pranav Shyam, Girish Sastry, Amanda Askell, et al. Language models are few-shot learners. *Advances in neural information processing systems*, 33:1877–1901, 2020.
- Mia Xu Chen, Orhan Firat, Ankur Bapna, Melvin Johnson, Wolfgang Macherey, George Foster, Llion Jones, Niki Parmar, Mike Schuster, Zhifeng Chen, et al. The best of both worlds: Combining recent advances in neural machine translation. *arXiv preprint arXiv:1804.09849*, 2018.
- Youngmin Cho and Lawrence Saul. Kernel methods for deep learning. *Advances in neural information processing systems*, 22, 2009.
- Alexis Conneau and Guillaume Lample. *Cross-Lingual Language Model Pretraining*. Curran Associates Inc., Red Hook, NY, USA, 2019.
- Hadi Daneshmand, Jonas Kohler, Francis Bach, Thomas Hofmann, and Aurelien Lucchi. Batch normalization provably avoids ranks collapse for randomly initialised deep networks. *Advances in Neural Information Processing Systems*, 33:18387–18398, 2020.
- Hadi Daneshmand, Amir Joudaki, and Francis Bach. Batch normalization orthogonalizes representations in deep random networks. *Advances in Neural Information Processing Systems*, 34, 2021.
- Jean Daunizeau. Semi-analytical approximations to statistical moments of sigmoid and softmax mappings of normal variables. *arXiv preprint arXiv:1703.00091*, 2017.
- Yihe Dong, Jean-Baptiste Cordonnier, and Andreas Loukas. Attention is not all you need: Pure attention loses rank doubly exponentially with depth. In *International Conference on Machine Learning*, pages 2793–2803. PMLR, 2021.

370 Alexey Dosovitskiy, Lucas Beyer, Alexander Kolesnikov, Dirk Weissenborn, Xiaohua Zhai, Thomas
371 Unterthiner, Mostafa Dehghani, Matthias Minderer, Georg Heigold, Sylvain Gelly, et al. An
372 image is worth 16x16 words: Transformers for image recognition at scale. *arXiv preprint*
373 *arXiv:2010.11929*, 2020.

374 Xavier Glorot and Yoshua Bengio. Understanding the difficulty of training deep feedforward neural
375 networks. In *Proceedings of the thirteenth international conference on artificial intelligence and*
376 *statistics*, pages 249–256. JMLR Workshop and Conference Proceedings, 2010.

377 Boris Hanin. Which neural net architectures give rise to exploding and vanishing gradients? *Advances*
378 *in neural information processing systems*, 31, 2018.

379 Boris Hanin and David Rolnick. How to start training: The effect of initialization and architecture.
380 *Advances in Neural Information Processing Systems*, 31, 2018.

381 Soufiane Hayou, Eugenio Clerico, Bobby He, George Deligiannidis, Arnaud Doucet, and Judith
382 Rousseau. Stable resnet. In *International Conference on Artificial Intelligence and Statistics*, pages
383 1324–1332. PMLR, 2021.

384 Kaiming He, Xiangyu Zhang, Shaoqing Ren, and Jian Sun. Delving deep into rectifiers: Surpassing
385 human-level performance on imagenet classification. In *Proceedings of the IEEE international*
386 *conference on computer vision*, pages 1026–1034, 2015.

387 Kaiming He, Xiangyu Zhang, Shaoqing Ren, and Jian Sun. Deep residual learning for image
388 recognition. In *IEEE Conference on Computer Vision and Pattern Recognition (CVPR)*, pages
389 770–778, 2016.

390 Sepp Hochreiter. Untersuchungen zu dynamischen neuronalen netzen. *Diploma, Technische Univer-*
391 *sität München*, 91(1), 1991.

392 Cheng-Zhi Anna Huang, Ashish Vaswani, Jakob Uszkoreit, Ian Simon, Curtis Hawthorne, Noam
393 Shazeer, Andrew M Dai, Matthew D Hoffman, Monica Dinulescu, and Douglas Eck. Music
394 transformer: Generating music with long-term structure. In *International Conference on Learning*
395 *Representations*, 2018.

396 Xiao Shi Huang, Felipe Perez, Jimmy Ba, and Maksims Volkovs. Improving transformer optimization
397 through better initialization. In *International Conference on Machine Learning*, pages 4475–4483.
398 PMLR, 2020.

399 Leon Isserlis. On a formula for the product-moment coefficient of any order of a normal frequency
400 distribution in any number of variables. *Biometrika*, 12(1/2):134–139, 1918.

401 Diederik P Kingma and Jimmy Ba. Adam: A method for stochastic optimization. *arXiv preprint*
402 *arXiv:1412.6980*, 2014.

403 Liyuan Liu, Haoming Jiang, Pengcheng He, Weizhu Chen, Xiaodong Liu, Jianfeng Gao, and
404 Jiawei Han. On the variance of the adaptive learning rate and beyond, 2019. URL <https://arxiv.org/abs/1908.03265>.
405

406 Liyuan Liu, Xiaodong Liu, Jianfeng Gao, Weizhu Chen, and Jiawei Han. Understanding the difficulty
407 of training transformers. *arXiv preprint arXiv:2004.08249*, 2020.

408 Ilya Loshchilov and Frank Hutter. Decoupled weight decay regularization. *arXiv preprint*
409 *arXiv:1711.05101*, 2017.

410 Jan R Magnus and Heinz Neudecker. *Matrix differential calculus with applications in statistics and*
411 *econometrics*. John Wiley & Sons, 2019.

412 Ido Nachum, Jan Hązła, Michael Gastpar, and Anatoly Khina. A johnson–lindenstrauss framework
413 for randomly initialized cnns. *arXiv preprint arXiv:2111.02155*, 2021.

414 XuanLong Nguyen, Martin J Wainwright, and Michael I Jordan. Estimating divergence functionals
415 and the likelihood ratio by convex risk minimization. *IEEE Transactions on Information Theory*,
416 56(11):5847–5861, 2010.

417 Lorenzo Noci, Gregor Bachmann, Kevin Roth, Sebastian Nowozin, and Thomas Hofmann. Precise
418 characterization of the prior predictive distribution of deep relu networks. *Advances in Neural*
419 *Information Processing Systems*, 34, 2021.

420 Antonio Orvieto, Jonas Kohler, Dario Pavlo, Thomas Hofmann, and Aurelien Lucchi. Vanishing
421 curvature and the power of adaptive methods in randomly initialized deep networks. *AISTATS*
422 *2022 (to appear)*, 2021.

423 Myle Ott, Sergey Edunov, Alexei Baevski, Angela Fan, Sam Gross, Nathan Ng, David Grangier,
424 and Michael Auli. fairseq: A fast, extensible toolkit for sequence modeling. In *Proceedings of*
425 *NAACL-HLT 2019: Demonstrations*, 2019.

426 Kishore Papineni, Salim Roukos, Todd Ward, and Wei-Jing Zhu. Bleu: a method for automatic
427 evaluation of machine translation. In *Proceedings of the 40th annual meeting of the Association*
428 *for Computational Linguistics*, pages 311–318, 2002.

429 Jeffrey Pennington, Samuel Schoenholz, and Surya Ganguli. Resurrecting the sigmoid in deep
430 learning through dynamical isometry: theory and practice. In I. Guyon, U. Von Luxburg, S. Bengio,
431 H. Wallach, R. Fergus, S. Vishwanathan, and R. Garnett, editors, *Advances in Neural Information*
432 *Processing Systems*, volume 30. Curran Associates, Inc., 2017. URL [https://proceedings.](https://proceedings.neurips.cc/paper/2017/file/d9fc0cdb67638d50f411432d0d41d0ba-Paper.pdf)
433 [neurips.cc/paper/2017/file/d9fc0cdb67638d50f411432d0d41d0ba-Paper.pdf](https://proceedings.neurips.cc/paper/2017/file/d9fc0cdb67638d50f411432d0d41d0ba-Paper.pdf).

434 Stanislas Polu, Jesse Michael Han, Kunhao Zheng, Mantas Baksys, Igor Babuschkin, and Ilya
435 Sutskever. Formal mathematics statement curriculum learning. *arXiv preprint arXiv:2202.01344*,
436 2022.

437 Ben Poole, Subhaneil Lahiri, Maithra Raghu, Jascha Sohl-Dickstein, and Surya Ganguli. Exponential
438 expressivity in deep neural networks through transient chaos. *Advances in neural information*
439 *processing systems*, 29, 2016.

440 Colin Raffel, Noam Shazeer, Adam Roberts, Katherine Lee, Sharan Narang, Michael Matena, Yanqi
441 Zhou, Wei Li, and Peter J Liu. Exploring the limits of transfer learning with a unified text-to-text
442 transformer. *arXiv preprint arXiv:1910.10683*, 2019.

443 Andrew M Saxe, James L McClelland, and Surya Ganguli. Exact solutions to the nonlinear dynamics
444 of learning in deep linear neural networks. *arXiv preprint arXiv:1312.6120*, 2013.

445 Samuel S. Schoenholz, Justin Gilmer, Surya Ganguli, and Jascha Sohl-Dickstein. Deep information
446 propagation. In *ICLR*, 2017.

447 Alexander Shekhovtsov and Boris Flach. Feed-forward propagation in probabilistic neural networks
448 with categorical and max layers. In *International conference on learning representations*, 2018.

449 Sidak Pal Singh, Gregor Bachmann, and Thomas Hofmann. Analytic insights into structure and
450 rank of neural network hessian maps. In A. Beygelzimer, Y. Dauphin, P. Liang, and J. Wortman
451 Vaughan, editors, *Advances in Neural Information Processing Systems*, 2021. URL [https:](https://openreview.net/forum?id=otDgw7LM7Nn)
452 [//openreview.net/forum?id=otDgw7LM7Nn](https://openreview.net/forum?id=otDgw7LM7Nn).

453 Ashish Vaswani, Noam Shazeer, Niki Parmar, Jakob Uszkoreit, Llion Jones, Aidan N Gomez, Lukasz
454 Kaiser, and Illia Polosukhin. Attention is all you need. *arXiv preprint arXiv:1706.03762*, 2017.

455 Hongyu Wang, Shuming Ma, Li Dong, Shaohan Huang, Dongdong Zhang, and Furu Wei. Deepnet:
456 Scaling transformers to 1,000 layers. *arXiv preprint arXiv:2203.00555*, 2022.

457 Qiang Wang, Bei Li, Tong Xiao, Jingbo Zhu, Changliang Li, Derek F Wong, and Lidia S Chao.
458 Learning deep transformer models for machine translation. *arXiv preprint arXiv:1906.01787*,
459 2019.

460 Lechao Xiao, Yasaman Bahri, Jascha Sohl-Dickstein, Samuel Schoenholz, and Jeffrey Penning-
461 ton. Dynamical isometry and a mean field theory of CNNs: How to train 10,000-layer
462 vanilla convolutional neural networks. In Jennifer Dy and Andreas Krause, editors, *Proceed-*
463 *ings of the 35th International Conference on Machine Learning*, volume 80 of *Proceedings*
464 *of Machine Learning Research*, pages 5393–5402. PMLR, 10–15 Jul 2018. URL [https:](https://proceedings.mlr.press/v80/xiao18a.html)
465 [//proceedings.mlr.press/v80/xiao18a.html](https://proceedings.mlr.press/v80/xiao18a.html).

- 466 Ruibin Xiong, Yunchang Yang, Di He, Kai Zheng, Shuxin Zheng, Chen Xing, Huishuai Zhang,
467 Yanyan Lan, Liwei Wang, and Tieyan Liu. On layer normalization in the transformer architecture.
468 In *International Conference on Machine Learning*, pages 10524–10533. PMLR, 2020.
- 469 Zhilin Yang, Zihang Dai, Yiming Yang, Jaime Carbonell, Russ R Salakhutdinov, and Quoc V Le.
470 Xlnet: Generalized autoregressive pretraining for language understanding. *Advances in neural*
471 *information processing systems*, 32, 2019.
- 472 Jacob Zavatone-Veth and Cengiz Pehlevan. Exact marginal prior distributions of finite bayesian
473 neural networks. *Advances in Neural Information Processing Systems*, 34, 2021.
- 474 Hongyi Zhang, Yann N Dauphin, and Tengyu Ma. Fixup initialization: Residual learning without
475 normalization. *arXiv preprint arXiv:1901.09321*, 2019.
- 476 Jingzhao Zhang, Sai Praneeth Karimireddy, Andreas Veit, Seungyeon Kim, Sashank Reddi, Sanjiv
477 Kumar, and Suvrit Sra. Why are adaptive methods good for attention models? *Advances in Neural*
478 *Information Processing Systems*, 33:15383–15393, 2020.

- 479 1. For all authors...
- 480 (a) Do the main claims made in the abstract and introduction accurately reflect the paper's
- 481 contributions and scope? [Yes]
- 482 (b) Did you describe the limitations of your work? [Yes] See Section 3
- 483 (c) Did you discuss any potential negative societal impacts of your work? [N/A]
- 484 (d) Have you read the ethics review guidelines and ensured that your paper conforms to
- 485 them? [Yes]
- 486 2. If you are including theoretical results...
- 487 (a) Did you state the full set of assumptions of all theoretical results? [Yes] See Section 3
- 488 (b) Did you include complete proofs of all theoretical results? [Yes] Most of them in the
- 489 Appendix
- 490 3. If you ran experiments...
- 491 (a) Did you include the code, data, and instructions needed to reproduce the main experi-
- 492 mental results (either in the supplemental material or as a URL)? [Yes] The code will
- 493 be released upon acceptance.
- 494 (b) Did you specify all the training details (e.g., data splits, hyperparameters, how they
- 495 were chosen)? [Yes] See Appendix.
- 496 (c) Did you report error bars (e.g., with respect to the random seed after running experi-
- 497 ments multiple times)? [Yes]
- 498 (d) Did you include the total amount of compute and the type of resources used (e.g., type
- 499 of GPUs, internal cluster, or cloud provider)? [Yes]
- 500 4. If you are using existing assets (e.g., code, data, models) or curating/releasing new assets...
- 501 (a) If your work uses existing assets, did you cite the creators? [N/A]
- 502 (b) Did you mention the license of the assets? [N/A]
- 503 (c) Did you include any new assets either in the supplemental material or as a URL? [N/A]
- 504
- 505 (d) Did you discuss whether and how consent was obtained from people whose data you're
- 506 using/curating? [N/A]
- 507 (e) Did you discuss whether the data you are using/curating contains personally identifiable
- 508 information or offensive content? [N/A]
- 509 5. If you used crowdsourcing or conducted research with human subjects...
- 510 (a) Did you include the full text of instructions given to participants and screenshots, if
- 511 applicable? [N/A]
- 512 (b) Did you describe any potential participant risks, with links to Institutional Review
- 513 Board (IRB) approvals, if applicable? [N/A]
- 514 (c) Did you include the estimated hourly wage paid to participants and the total amount
- 515 spent on participant compensation? [N/A]